analytical chemistry

Article

pubs.acs.org/ac

Computed Molecular Depth Profile for C_{60} Bombardment of a Molecular solid

Robert J. Paruch,[†] Barbara J. Garrison,*[,†] and Zbigniew Postawa*[,‡]

[†]Department of Chemistry, Penn State University, 104 Chemistry Building, University Park, Pennsylvania 16802, United States

[‡]Smoluchowski Institute of Physics, Jagiellonian University, ul. Reymonta 4, 30-059 Krakow, Poland

Supporting Information

ABSTRACT: Molecular dynamics (MD) simulations have been performed for 10 keV C_{60} bombardment of an octane molecular solid at normal incidence. The results are analyzed using the steady-state statistical sputtering model (SS-SSM) to understand the nature of molecular motions and to predict a depth profile of a δ-layer. The octane system has sputtering yield of ~150 nm^3 of which 85% is in intact molecules and 15% is fragmented species. The main displacement mechanism is along the crater edge. Displacements between layers beneath the impact point are difficult because the nonspherically shaped octane molecule needs a relatively large volume to move into and the molecule needs to be aligned properly for the displacement. Since interlayer mixing is difficult, the predicted depth profile is dominated by the rms roughness and the large information depth because of the large sputtering yield.

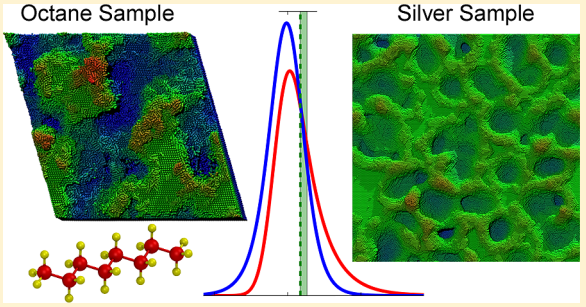

A unique aspect of cluster secondary ion mass spectrometry (SIMS) is the ability to depth profile through a molecular solid with chemical specificity.[1−3] There are systems for which depth profiling works well, such as trehalose, Irganox, cholesterol, Langmuir−Blodgett films, amino acids, and organic light emitting diodes (OLEDs) if the metal overlayer is delaminated first. Challenges do arise in depth profiling of some polymers[4] and in heterogeneous systems, such as metal overlayers on organic solids[5,6] or prefabricated metal−organic systems.[7] In addition, some systems exhibit a temperature effect in which the depth profile quality is significantly enhanced by cooling the sample.[2,3] These temperature effects clearly indicate that there is a long time scale process taking place in addition to the beam induced effects.

Regardless of the difficulties associated with some systems, there is the class of molecular solids that depth profile with relative ease. Given the enormous energy of the incident cluster projectile relative to the cohesive energy of the molecular solid and the bond strengths within individual molecules, it remains somewhat surprising that depth profiling actually does work.

A protocol to model the depth profiling process has been developed[8] and to date applied to atomic solids of metals[9−13] and silicon.[14] Although some aspects of the depth profiling process, such as considerable lateral motion in addition to vertical displacements[8,13,15] and the importance of the sputtering yield versus the displacement yield[11] are emerging, questions that involve chemical damage and interlayer mixing of the nonspherically shaped organic molecules remain. In this study, we present the findings of using an analytic model to interpret the results of repetitive bombardment simulations of an octane molecular solid by 10 keV C_{60} in the contexts of depth profiling. The simulations show clearly that it is difficult for molecules to undergo interlayer mixing below the impact point, a new concept to understanding bombardment of molecular solids. As a result, the simulations predict a symmetrical depth profile of a δ-layer shifted toward the surface from the actual δ-layer position.

SIMULATION AND MODEL

The molecular dynamics (MD) approach for modeling repetitive energetic cluster bombardment using the "divide and conquer" protocol has been described previously.[8,11,12] Briefly, a master crystal is created that is sufficiently large to allow for development of topography. Each projectile impact is calculated using a subsystem of the atoms. After the MD calculation is finished, the subsystem is reinserted into the master crystal. A recent modification of the computer code[16] to implement the parallel messaging passing interface (MPI) now allows us to perform repetitive bombardment simulations on a molecular solid (octane, C_8H_{18}) using an atomistic interaction potential, AIREBO.[17] As the model sample for molecular depth profiling simulations we chose an octane crystal. Octane solid forms in a triclinic structure.[18] We do consider the sample to be a representative molecular solid and consequently only make conclusions from the simulations that we believe to be general and not specific to the octane molecule. In our simulations, the main axis of the molecule is oriented along the surface normal, thus the molecules make layers 1.09 nm deep. The master

Received: September 23, 2013
Accepted: November 5, 2013
Published: November 5, 2013

crystal for the simulations is a parallelogram of 37 nm on a side with a total surface area of 1400 nm^2 and a depth of 40 nm. The master crystal consists of 7 684 794 atoms or 295 569 octane molecules.

The projectile for the simulations is C_{60} bombarding with 10 keV kinetic energy at normal incidence. These conditions were chosen as a reasonable compromise between actual experimental conditions and computational tractability. For this projectile and energy, the subsystem size used for each impact is a cylinder of radius 12 nm capped at the bottom by a hemisphere. The hemispherical part of the sample begins at the depth of the deepest valley near the impact point to ensure that there is sufficient material to contain the initial kinetic energy. As a result, the cylinder is 0−8 nm deep depending on the local topography. There are 450 000−800 000 atoms in each subsystem. The simulation time for each impact is 35 ps. A few single impact simulations with C_{60} aimed at selected topology structures have been run up to 43 ps to check if 35 ps is still sufficient to properly describe sputtering events during development of surface morphology, and to probe the effect of projectile impact on various morphological structures. The simulations were run on the lion-xg cluster[19] on 9 processors, taking 4−12 days per impact. For comparison, an impact of C_{60} on Ag can be run in a handful of hours on one processor.

The atomistic AIREBO potential is used for the simulations.[17] It describes respectably well reactions among hydrocarbon species,[20] in particular, dissociation and H addition and abstraction. Of note is that octane is a saturated hydrocarbon molecule with no readily available opportunity for cross-linking.

The quantitative analysis of the sputtering and displacement of molecules is performed using the steady-state statistical sputtering model (SS-SSM).[11,12] The SS-SSM characterizes the sputtering and displacement distributions and connects them with depth profile quality of a δ-layer. The essential quantities in the model come from the results of the MD simulations. The distribution of number of atoms sputtered from each sample layer and the number of particles (atoms or molecules, depending on the system) displaced from one layer to another obtained from the MD simulation are the essential inputs to the SS-SSM. The key connection between the MD simulations and the SS-SSM quantities is the evaluation of the sputtering, Γ_j, and the displacement, $\Delta_{j\rightarrow j'}$, terms. The sputtering parameter in its raw form Γ_j denotes the average number of particles sputtered from the j-th system layer per impact, where $j = 0$ represents the average surface level, $j < 0$ and $j > 0$ represent the layers above and below the average surface level, respectively. The displacement parameter $\Delta_{j\rightarrow j'}$ denotes the average number of atoms relocated from the j-th to j'-th system layer per impact. It describes the displacement of the sample material in the vertical direction that is in the direction perpendicular to the original flat sample surface. Interchangeably, we use the term "interlayer mixing" for this type of displacement. The sum of Γ_j over all j values gives the total sputtering yield. Correspondingly, we have defined a total displacement yield that is the sum of $\Delta_{j\rightarrow j'}$ over all j and j' values.[11] The total displacement yield does depend on the thickness of the layers in the system and thus does not have a well-defined value. It is, however, a very convenient means of condensing the amount of displacement in a system into a single quantity.

RESULTS

The results of the simulation of repetitive bombardment of C_{60} on octane are presented in the following order. First, the sputtering yield and roughness will be discussed followed by the sputtering and displacement distributions, sample motions, and the importance of fragmentation or chemical damage. Finally, the depth profile will be presented.

A total of 54 impacts, which correspond to the projectile fluence of $3.9 \times 10^{12}/cm^2$, have been performed over a 16 month period. The last ten impacts are used for analysis. We have been carefully monitoring the changes in the results as more impacts have been computed. The quantities of sputtering yield and rms roughness are increasing and the fraction of sputtered fragments is decreasing. The amount of fragmented species remaining in the solid is relatively constant. We have been cautious with our interpretations and feel that the conclusions presented are sound.

For discussion, a comparison of the values of yield, surface roughness, and sputtering and displacement distributions to those from C_{60} bombardment of Ag at 20 keV at normal incidence[11,12] is made. This system was chosen because the sputtering and displacement yields are both large among the calculations with a silver sample we have performed to date. The differences between the systems are illustrative for understanding the values obtained in this simulation. Of note is that the results and conclusions are for a loosely bound solid of relatively small molecules when compared to firmly bound macromolecular solids such as polymers.[21] However, some general predictions will also hold in those materials.

Yields and Roughness. The calculated total sputtering yield for the octane system is 147 nm^3 per incident C_{60}. This volume corresponds to 693 molecular equivalents using the molecule volume in the simulation system of 0.212 nm^3. For comparison, experimental values of sputtering yield of trehalose[22] sputtered by C_{60} with 20 keV incident energy at an angle of 40° is 87 nm^3 and for cholesterol for 40 keV C_{60} at 40° incidence is 274 nm^3.[23−25] The reported values of the sputtering yields for 10 keV C_{60} at 40° bombardment of Irganox 1010 and Irganox 3114 samples are 82 ± 8 and 92 ± 9 nm^3, respectively,[26] and from 120 to 300 nm^3 for the Irganox 1010/3114 δ-layer sample sputtered by 40 keV C_{60}.[27] For comparison, the calculated yield[9,11,12] for 20 keV C_{60} bombardment of Ag is 6.4 nm^3, and the experimental value[28] for 20 keV C_{60} bombardment of Au is 2.2 nm^3. In general, the calculated sputtering yield for the octane system is reasonable with respect to the experimental values of molecular systems and is much larger than the sputtering yields of metals.

The rms roughness for the octane system is 3.3 nm. Of note is that for the performed number of impacts the rms roughness is still increasing. The results of the simulation were interpreted with the SS-SSM model assuming that the surface roughness does not change significantly when depth profiling through the width of the δ-layer.[26] For comparison, the steady-state rms roughness for 20 keV C_{60} bombardment of Ag is 2.4 nm.[9,11,12] As discussed below, the octane roughness is due primarily to a large sputtering yield that forms big craters in contrast to the Ag system where most of the roughness is from displacements and moving material around.

Sputtering and Displacement Distributions. The sputtering (Γ) and displacement (Δ) distributions for intact octane molecules are shown in Figure 1a. All distributions are in units of volume (nm^3) versus the layer number, where $j = 0$

dx.doi.org/10.1021/ac403035a | Anal. Chem. 2013, 85, 11628−11633

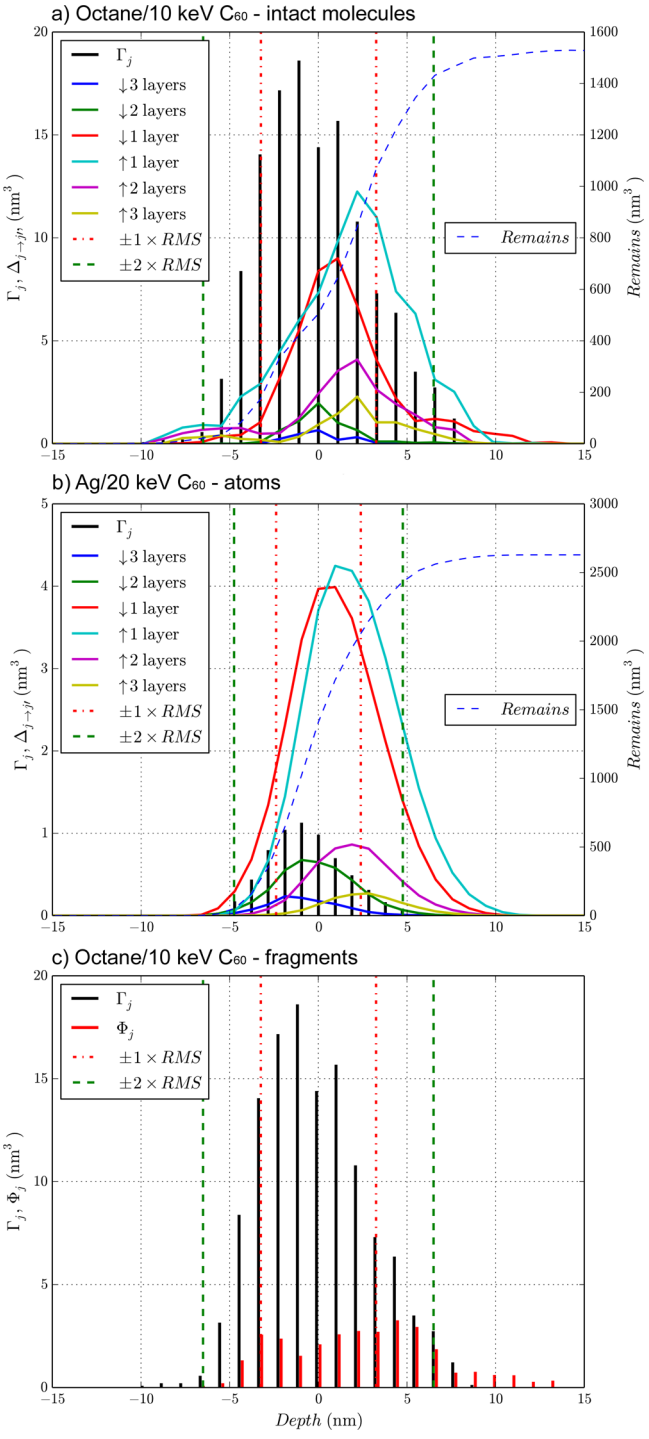

Figure 1. Sputtering (Γ) and displacement (Δ) distributions for (a) 10 keV C_{60} bombardment of an octane sample and (b) 20 keV C_{60} bombardment of an Ag sample. (c) The depth distribution of where the octane molecules are fragmented (Φ) along with the sputtering distribution reproduced from panel a. The red and green vertical dashed lines correspond to ±1 and ±2 × rms roughness depths, respectively. The sigmoidal dashed blue line gives the fraction of a layer that remains in the layer and is not sputtered or displaced.

corresponds to the average surface level. The layers are 1.09 nm thick which corresponds to the thickness of the molecular layer. The sputtering yields are given by the black bars. The displacement yields are given by lines with, for example, moving up one layer shown in cyan and moving down one layer shown in red. The width of the sputtering and displacement distributions span approximately the distance from −2 × rms roughness (the peaks of the roughened surface) to +2 × rms roughness (the valleys of the roughened surface). All of the interlayer mixing is occurring within the roughened surface and there is no accumulation of interlayer mixing below it. As a result, simplistically, the interlayer mixing can be removed in a single impact. The sputtering yield of intact molecules is 125 nm^3 or about 70% of the displacement yield of intact molecules of 176 nm^3 for the layer thickness assumed in the analysis. Compared to metal systems, not only is the yield large but also the ratio of the sputtering to displacement yield is larger.[11] Generally, both the factors of displacements within the roughened surface and the large sputtering to displacement yield ratio are favorable for quality of depth profiles.

The distributions for C_{60} bombardment of Ag at 20 keV are given in Figure 1b.[11,12] The layer widths used for analysis are four atomic layers or 0.94 nm. In this case, the sputtering distribution does not extend to the bottom of the valleys. As discussed below, the cohesive energy is sufficiently large that it traps the atoms within the valley before they sputter. On the other hand, the displacement distribution extends well beyond them, thus there is accumulation of interlayer mixing below the roughened surface. The total sputtering yield is 6.4 nm^3 or less than 10% of the total displacement yield of 71 nm^3. In general, both conditions are not as favorable as the ones for octane for depth profiling. Both of these factors are discussed below in conjunction with the depth profiles.

The differences in the two systems can be qualitatively analyzed using the mesoscale energy deposition footprint (MEDF) model developed previously.[29,30] The majority of the primary kinetic energy of the projectile is deposited into the system within the first 50−150 fs.[29−32] In this time regime, the C_{60} projectile acts as a single particle experiencing frictional forces.[33,34] The deposited energy is within a mini-track-like region of a given radius as determined from the MD simulations. The volume from which the material ejects is proportional to the radius of the track raised to the third power and to the ratio of the energy density divided by the cohesive energy. This model is only applicable to atomic-like solids since it does not account for the energy deposited into fragmentation events but still gives qualitative insight. The track radii are similar for three systems C_{60} at 15 keV on Ag,[32] C_{60} at 10−20 keV on rigid water,[30] and C_{60} at 20 keV on octane[31] given radii of 1.8 nm, 2.4−2.6 and 2 nm, respectively. Since the projectile energy is deposited within approximately the same region for both octane and Ag, the differences between the sputtering and displacement distributions must be explained by partitioning of this energy between sputtering and displacements. For the Ag sample, the cohesive energy per atom (2.95 eV) calculated from the MD/MC-CEM potential[35] is relatively large. Thus, the whole energized volume cannot be sputtered even though there is sufficient energy to displace atoms between layers beneath the impact position. With the use of the AIREBO interaction potential,[31] the cohesive energy of the octane solid is 0.63 eV per molecule thus it is easier energetically to sputter the molecules in the energized region than in the Ag system. For the atomic solid, the volume that has to be available for the atom to move into an adjacent layer is relatively small. Moreover, there is no orientational alignment that the atom needs to make in order to move. For the molecular solid, on the other hand, a larger volume needs to be available for the displacement of molecular species and the molecule needs to be

dx.doi.org/10.1021/ac403035a | Anal. Chem. 2013, 85, 11628−11633

aligned properly with velocity in the correct direction. Thus, interlayer displacements below the impact point are difficult for the molecular system because there is not available free volume for the move. Such a type of displacement is much easier in the presence of molecular fragmentation.[26] As discussed later, however, in the investigated system we see little damage. Consequently, as can be seen in the animations discussed in the following section, most of the displacements for octane are along the crater edge.

Motions. Three impacts are chosen for illustration of C_{60} bombardment on a roughened octane surface. The first impact is on the top of a hill, the second on the side of a hill and the last directly in a valley as shown in Figure 2 and Supporting

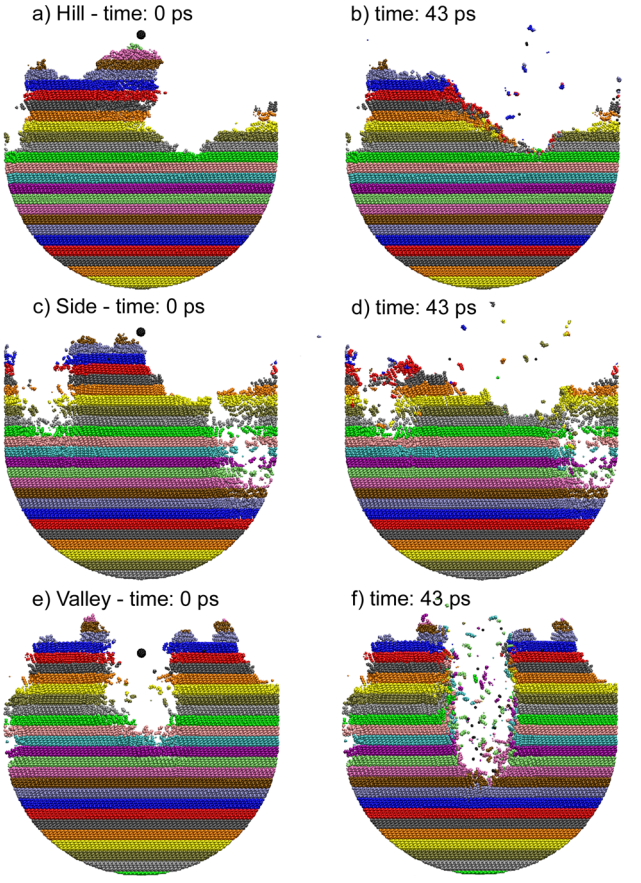

Figure 2. Cross sectional view of an initial and final state of an octane subsystem used for MD calculations being bombarded by 10 keV C_{60}, where the projectile is aimed at (a, b) the top of a hill, (c, d) the side of a hill, and (e, f) the bottom of a valley. The samples are colored according to the molecular layers of thickness 1.09 nm. The projectile is colored black.

Information Animations 1−3. The before and after snapshots in Figure 2 show the lack of interlayer mixing below the impact point as discussed above. The animations show that the molecules can easily be displaced only along the crater edge into empty spaces created by the same impact or along the edge of the roughened surface into preexisting empty spaces, created by previous impacts. This motion is quite apparent for the impact in the bottom of the valley (Figure 2e, f and Supporting Information Animation 3) where there is almost a jetting type motion[5] with molecules streaming up the sides of the pit. In fact, this type of motion allows the molecules to traverse a relatively large distance compared with the distance of interlayer mixing, where the molecules travel only between a layer and the adjacent ones. Analogous animations for an Ag system have been published previously.[8]

Fragmentation. The final channel to assess is chemical fragmentation or damage. The MD simulations describe direct bond cleavage, H-abstraction reactions and cross-linking events during the time scale of an impact.[20,36] The simulations do not include long time scale events such as those involved in the observed temperature effects.[2,3] Because octane is a saturated hydrocarbon molecule there is minimal opportunity for cross-linking, thus by chemical damage we are referring to fragmentation of the molecules.

The total chemical damage yield is 30 nm^3 per incident C_{60} of which 22 nm^3 is sputtered and 8 nm^3 remains in the sample. The depth distribution of where the molecules are damaged is shown in Figure 1c along with the sputtering distribution reproduced from Figure 1a. The chemical damage (Φ) overlaps with the sputtering region but also extends five nm into the solid, indicating that some chemical damage is accumulating. The possible explanation of the damage creation below the roughened surface is that small fragments either from the projectile or an octane molecule penetrate the solid and eventually fragment a molecule relatively deep below the impact point. Previous simulations[31,37] show that the damage region is directly below the impact in the mini-track-like region described in the MEDF model and is created in the very early stages of the impact event. Overall, of the sputtered material, ∼85% is in intact molecules and ∼15% in fragmented material. Simulations we have performed for C_{60} bombardment on flat surfaces of octane and octatetraene as a function of incident energy show that both the sputtering yield and the damage yield increase proportionately with increasing impact energy.

The impact from Figure 2c, d has been recolored to show intact and fragmented molecules in Figure 3 and Supporting

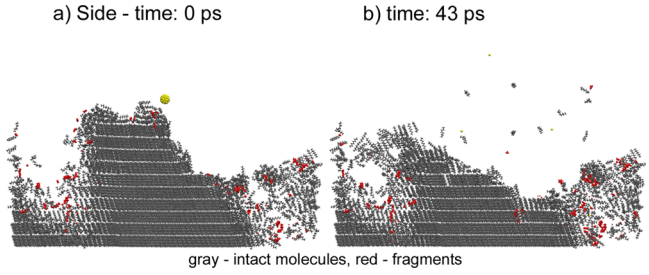

Figure 3. Snapshots of the bombardment event from Figure 2c, d recolored to show intact, gray, and fragmented, red, octane molecules. The projectile is colored yellow.

Information Animation 4. In Figure 3a, it is clear that the leftover fragments are in the crater regions of previous impacts as has also been observed for C_{60} bombardment of benzene on flat surfaces.[38] The final frame in Figure 3b shows additional fragments created by the impact, some being sputtered and some implanted in the near surface region. It also shows that because the fragments are created very early in the impact event and in a very energized region, they tend to eject early in the process and not to accumulate in the sample.

Depth Profile. The predicted depth profile of an octane δ-layer for intact molecules as well as the depth profile for the Ag δ-layer are given in Figure 4. The full procedure for converting the raw SS-SSM data into the smooth Dowsett function has been described previously.[12] The thicknesses of δ-layers are

dx.doi.org/10.1021/ac403035a | Anal. Chem. 2013, 85, 11628−11633

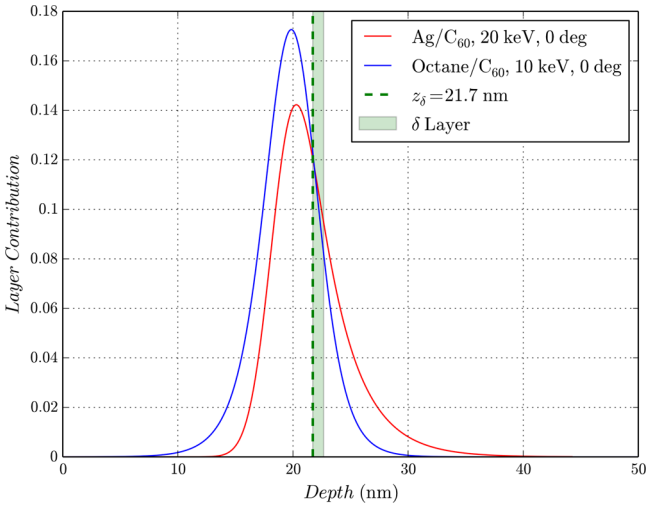

Figure 4. Depth profiles of a δ-layer for 10 keV C_{60} bombardment of an octane sample and 20 keV C_{60} bombardment of an Ag sample. The vertical green bar shows the position of the δ-layer in the sample.

equal to 1.09 and 0.94 nm, respectively for the two systems. The calculated full width at half-maximum (fwhm) for the octane δ-layer depth profile is 5.5 nm. For comparison, experimental values of fwhm for low temperature conditions for the Irganox 1010/3114 δ-layer sample sputtered by 40 keV C_{60} at 40°, where the δ-layer thicknesses vary from 3.0 to 3.7 nm, are from 17 to 22 nm,[27] and for a 4.4 nm lipid δ-layer depth profiled by 20 keV C_{60} at 71°, the fwhm is 12.1 ± 0.9 nm.[39] The predicted fwhm of the octane δ-layer is sensible with regard to the experimental results for molecular solids.

The depth profiles reflect several factors including the surface roughness, the interlayer mixing and the information depth of sputtering from individual impacts.[40,41] The effect of the roughened surface is present in both systems and will be discussed first. The interlayer mixing and information depth effects will be discussed next.

The roughened surface extends a distance of approximately ±2 × rms roughness from the average surface level. Thus, assuming particles only sputter from the surface edge of the roughened surface, the particles sputtered from the δ-layer will first appear in the depth profile at a depth 2 × rms roughness before the δ-layer position and will extend 2 × rms roughness below the δ-layer position. In this scenario, the depth profile will be symmetrical and centered at the δ-layer position.[12] The rms roughness contributes only to the width of the depth profile. The rms roughness for the octane system is approximately 3.3 nm and for the Ag system is 2.4 nm, two values sufficiently similar that the widths of the calculated depth profiles in Figure 4 appear similar.

There is an effect that contributes to the depth profile width and can also shift its peak position toward the sample surface, relative to the δ-δ-layer location. The interlayer mixing below the roughened surface pushes material from the δ-layer both up and down. The material pushed up makes the peak position appear closer to the surface and the material pushed down creates a trailing tail in the depth profile. Finally, there is the information depth that is the average depth of material removed in individual impact. The information depth is encoded in the sputtering distribution (Γ) albeit convoluted with the surface roughness. If contribution of the interlayer mixing to the depth profile is relatively low, the effect of information depth shows as an asymmetrical depth profile with longer leading tail. The final shape of the depth profile is an interplay of the effects of the surface roughness, interlayer mixing and information depth.

The importance of interlayer mixing on the depth profiles can be easily determined from the SS-SSM calculations by omitting the interlayer mixing terms (Δ terms) in the model equations. As shown previously,[12,14] if the interlayer mixing is omitted for the Ag system, then the depth profile is almost symmetrical and centered at the δ-layer position. Thus, the shift in peak position and the asymmetrical tail in the Ag depth profile is due to interlayer mixing. It is clear from Figure 1b that there is significant interlayer mixing below the region where sputtering occurs. The result of omitting the interlayer mixing in model calculations for the octane system is that the initial asymmetry of the depth profile with longer leading tail becomes even more apparent and the peak shift is reduced. From the results of individual bombardments of a flat surface we can estimate the information depth to be ~3 nm for the octane system and only ~1 nm for the Ag one. The difference is mostly caused by various binding energies of these solids. Thus, the asymmetry of depth profile for the octane system is mainly created by the information depth. The distributions given in Figure 1a show that all interlayer mixing in the octane system is in the roughened surface, from which the particles are sputtered, so its effective contribution to the depth profile is weak.

The two depth profiles in Figure 4 open the door for discussion of which is better. The depth profile for the octane system has a fwhm value of 5.5 nm vs the calculated fwhm of the silver δ-layer depth profile of 6.4 nm,[11] thus the depth profile for the organic system is narrower. On the other hand, the Ag distribution even with the asymmetrical tail has a peak position closer to the actual δ-layer position. The narrower width will result in better depth resolution of the depth profile, while the peak position closer to the actual δ-layer position will result in a better δ-layer localization in the sample.

The language of the discussion here and previous studies of depth profiling[40,41] treat the three physical factors that influence the depth profile, namely information depth, surface roughness and interlayer mixing as independent entities. What is clear from the simulations, however, is that the rms roughness depends on the information depth and the interlayer mixing. In the case of the octane system, the large information depth (which is related to large sputtering yield) is the cause of the rms roughness. In the case of the Ag system, where information depth is relatively small but the displacement yield is high the rms roughness correlates strongly with the displacement yield or the amount of interlayer mixing.[11]

CONCLUSIONS

Molecular dynamics simulations have been performed to model repetitive bombardment of an organic solid of octane molecules by C_{60} projectiles. Because of the relatively small cohesive energy compared with, for example, metals, the total sputtering yield is high, ~150 nm^3. Of the total sputtering yield, approximately 85% is in intact molecules and the remainder in fragments. The amount of fragments left in the solid is about one-third of the amount of ejected fragments. This large total sputtering yield is responsible for the roughness that develops on the surface. There are minimal interlayer displacements in the system beneath the impact point. The organic molecule needs a large volume to move into and needs to be properly

dx.doi.org/10.1021/ac403035a | Anal. Chem. 2013, 85, 11628−11633

aligned in order to move between layers. Virtually all the displacements occur along the crater edge and can be two to three nm in length. Since all the displacements are in the roughened surface region, the depth profile of a δ-layer is asymmetrical with longer leading edge because of a large information depth, which is related to the large sputtering yield for the molecular solid octane. The simulations have clearly identified the specific nature of mixing occurring in molecular solids and the effect of information depth, surface roughness and interlayer mixing, on the shape and position of the depth profile compared to the actual δ-layer position. They have also shown that these quantities are not independent.

■ ASSOCIATED CONTENT

Supporting Information

Animations showing bomardments of octane samples. This material is available free of charge via the Internet at http://pubs.acs.org.

■ AUTHOR INFORMATION

Corresponding Authors

*E-mail: bjg@psu.edu

*E-mail: zbigniew.postawa@uj.edu.pl.

Notes

The authors declare no competing financial interest.

■ ACKNOWLEDGMENTS

The authors gratefully acknowledge financial support from the Polish National Science Center, Program Nos. 2013/09/B/ST4/00094 and PB1839/B/H03/2011/40. We appreciate the support of the Penn State Research Computing and Cyberinfrastructure group in performing these simulations. The visualization of data presented in this paper was done with the matplotlib Python library[42] and the VMD program.[43]

■ REFERENCES

(1) Winograd, N. *Anal. Chem.* **2005**, *77*, 142A.

(2) Mahoney, C. M.; Wucher, A. In *Cluster Secondary Ion Mass Spectrometry Principles and Applications*; Mahoney, C. M., Ed.; John Wiley & Sons, Inc.: Hoboken, NJ, 2013, p 117.

(3) Shard, A.; Gilmore, I. S.; Wucher, A. In *TOF-SIMS: Materials Analysis by Mass Spectrometry*, 2nd ed.; Vickerman, J. C., Briggs, D., Eds.; IMP and SurfaceSpectra, Ltd.: Chichester, U.K., and Manchester, U.K., 2013.

(4) Mahoney, C. M. *Mass Spectrom. Rev.* **2009**, *29*, 247.

(5) Kennedy, P. E.; Postawa, Z.; Garrison, B. J. *Anal. Chem.* **2013**, *85*, 2348.

(6) Cheng, J.; Winograd, N. *Appl. Surf. Sci.* **2006**, *252*, 6498.

(7) Wucher, A.; Cheng, J.; Winograd, N. *Anal. Chem.* **2007**, *79*, 5529.

(8) Russo, M. F.; Postawa, Z.; Garrison, B. J. *J. Phys. Chem. C* **2009**, *113*, 3270.

(9) Paruch, R.; Rzeznik, L.; Russo, M. F.; Garrison, B. J.; Postawa, Z. *J. Phys. Chem. C* **2010**, *114*, 5532.

(10) Postawa, Z.; Rzeznik, L.; Paruch, R.; Russo, M. F.; Winograd, N.; Garrison, B. J. *Surf. Interface Anal.* **2011**, *43*, 12.

(11) Paruch, R. J.; Garrison, B. J.; Postawa, Z. *Anal. Chem.* **2012**, *84*, 3010.

(12) Paruch, R. J.; Postawa, Z.; Wucher, A.; Garrison, B. J. *J. Phys. Chem. C* **2012**, *116*, 1042.

(13) Garrison, B. J.; Postawa, Z. *Chem. Phys. Lett.* **2011**, *506*, 129.

(14) Krantzman, K. D.; Wucher, A. *J. Phys. Chem. C* **2010**, *114*, 5480.

(15) Krantzman, K. D.; Cook, E. L.; Wucher, A.; Garrison, B. J. *Nucl. Instrum. Methods Phys. Res., Sect. B* **2011**, *269*, 1591.

(16) Garrison, B. J.; Postawa, Z. In *ToF-SIMS—Surface Analysis by Mass Spectrometry*, 2nd ed.; Vickerman, J. C., Briggs, D., Eds.; IMP and SurfaceSpectra Ltd: Chichester, U.K., and Manchester, U.K., 2013; p 151.

(17) Stuart, S. J.; Tutein, A. B.; Harrison, J. A. *J. Chem. Phys.* **2000**, *112*, 6472.

(18) Mathisen, H.; Norman, N.; Pedersen, B. F. *Acta Chem. Scand.* **1967**, *21*, 127.

(19) Penn State University RCC http://rcc.its.psu.edu/resources/hpc/lionxg/ (accessed 8/20/2013).

(20) Garrison, B. J.; Kodali, P. B. S.; Srivastava, D. *Chem. Rev.* **1996**, *96*, 1327.

(21) Delcorte, A.; Garrison, B. J. *J. Phys. Chem. C* **2007**, *111*, 15312.

(22) Wucher, A.; Cheng, J.; Winograd, N. *J. Phys. Chem. C* **2008**, *112*, 16550.

(23) Kozole, J.; Wucher, A.; Winograd, N. *Anal. Chem.* **2008**, *80*, 5293.

(24) Kozole, J.; Willingham, D.; Winograd, N. *Appl. Surf. Sci.* **2008**, *255*, 1068.

(25) Shen, K.; Mao, D.; Garrison, B. J.; Wucher, A.; Winograd, N. *Anal. Chem.* **2013**, *85*, 10565.

(26) Shard, A. G.; Green, F. M.; Brewer, P. J.; Seah, M. P.; Gilmore, I. S. *J. Phys. Chem. B* **2008**, *112*, 2596.

(27) Mao, D.; Lu, C. Y.; Winograd, N.; Wucher, A. *Anal. Chem.* **2011**, *83*, 6410.

(28) Yang, L.; Seah, M. P.; Anstis, E. H.; Gilmore, I. S.; Lee, J. L. S. *J. Phys. Chem. C* **2012**, *116*, 9311.

(29) Russo, M. F.; Garrison, B. J. *Anal. Chem.* **2006**, *78*, 7206.

(30) Russo, M. F.; Szakal, C.; Kozole, J.; Winograd, N.; Garrison, B. J. *Anal. Chem.* **2007**, *79*, 4493.

(31) Garrison, B. J.; Postawa, Z.; Ryan, K. E.; Vickerman, J. C.; Webb, R. P.; Winograd, N. *Anal. Chem.* **2009**, *81*, 2260.

(32) Czerwinski, B.; Rzeznik, L.; Stachura, K.; Paruch, R.; Garrison, B. J.; Postawa, Z. *Vacuum* **2008**, *82*, 1120.

(33) Garrison, B. J.; Ryan, K. E.; Russo, M. F.; Smiley, E. J.; Postawa, Z. *J. Phys. Chem. C* **2007**, *111*, 10135.

(34) Ryan, K. E.; Russo, M. F.; Smiley, E. J.; Postawa, Z.; Garrison, B. J. *Appl. Surf. Sci.* **2008**, *255*, 893.

(35) Kelchner, C. L.; Halstead, D. M.; Perkins, L. S.; Wallace, N. M.; Depristo, A. E. *Surf. Sci.* **1994**, *310*, 425.

(36) Brenner, D. W.; Shenderova, O. A.; Harrison, J. A.; Stuart, S. J.; Ni, B.; Sinnott, S. B. *J. Phys.: Condens. Matter* **2002**, *14*, 783.

(37) Ryan, K. E.; Wojciechowski, I. A.; Garrison, B. J. *J. Phys. Chem. C* **2007**, *111*, 12822.

(38) Kennedy, P. E.; Garrison, B. J. *Surf. Interface Anal.* **2013**, *45*, 42.

(39) Lu, C. Y.; Wucher, A.; Winograd, N. *Anal. Chem.* **2011**, *83*, 351.

(40) Dowsett, M. G.; Rowlands, G.; Allen, P. N.; Barlow, R. D. *Surf. Interface Anal.* **1994**, *21*, 310.

(41) Hofmann, S. *Surf. Interface Anal.* **2000**, *30*, 228.

(42) Hunter, J. D. *Comput. Sci. Eng.* **2007**, *9*, 90.

(43) Humphrey, W.; Dalke, A.; Schulten, K. *J. Mol. Graphics* **1996**, *14*, 33.